

Ferroelectricity of Ice Nanotubes inside Carbon Nanotubes

Chuanfu Luo, Wei Fa, and Jinming Dong*

Group of Computational Condensed Matter Physics,
National Laboratory of Solid State Microstructures and Department of Physics,
Nanjing University, Nanjing, 210093, People's Republic of China

(Dated: August 6, 2018)

We report that ice nanotubes with odd number of side faces inside carbon nanotubes exhibit spontaneous electric polarization along its axis direction by using molecular dynamics simulations. The mechanism of this nanoscale quasi-one-dimensional ferroelectricity is due to low dimensional confinement and the orientational order of hydrogen bonds. These ferroelectric fiber structural materials are different from traditional perovskite structural bulk materials.

PACS numbers: 77.84.-s, 85.35.Kt, 61.46.Fg, 68.08.De

Whether ferroelectric ice exists is a question that has long fascinated researchers[1, 2, 3, 4]. Although one water molecule has a significant dipole moment, normal hexagonal ice *Ih* does not possess ferroelectricity and it is very difficult to get an ice phase even with a weak whole polarization. Several year ago, the ferroelectricity of ice films grown on ultra-clean platinum was detected, although only a small proportion (0.2%) of the molecules are aligned[5, 6]. Most recently, Fukazawa *et al.* have succeeded in making Ice XI in the laboratory and suggests existence of ferroelectric ice in the universe[7].

Confinement of matter on the nanometer scale can induce phase transitions not seen in bulk systems [8, 9]. In biology as well as in natural and synthetic materials, water is often tucked away in tiny crevices inside proteins or in porous materials. Therefore, water confined in nanoscale quasi-one-dimensional (Q1D) channels is of great interest to biology, geology, and materials science. Recent investigations have increased our understanding of confined water, showing that, in nanoscopic proportions, many water properties differ drastically from those of bulk water [10, 11, 12]. In particular, an excellent model is water confined in carbon nanotubes, which have been adopted in many previous studies [13, 14, 15, 16, 17, 18, 19, 20, 21, 22, 23, 24, 25, 26]. Among these interesting investigations, Koga *et al.* investigated water inside single-walled carbon nanotubes (SWCNTs) of diameter 1.1~1.4 nm and found that water forms ice nanotubes composed by a rolled square ice sheet [14, 15, 16]. Recent neutron scattering studies, combined with molecular dynamics (MD) simulations, revealed that water in SWCNTs of diameter 1.4 nm forms a core-shell structure, in which the square ice sheet described by Koga *et al.* is coupled with a chainlike configuration at the center of the shell [27, 28].

Recently, investigations of nanoscale ferroelectric materials are very active due to its potential application [29, 30, 31]. Because of its particular structures, the ice nanotubes inside SWCNTs may exhibit ferroelectricity.

In this paper, we report that ice nanotubes with odd number of side faces inside SWCNTs exhibit spontaneous electric polarization along its axis direction by using MD simulations. The origin of ferroelectricity of these ice nanotubes is due to the strong direction preferred hydrogen-bonds between water molecules and the Q1D confinement inside SWCNTs, which is different from traditional ferroelectric bulk materials, such as displacive perovskite-based oxides.

The water-water interaction is modelled by the TIP4P model [32], which has been used in many simulations and given theoretical results in well consistent with experiments [10, 13, 14, 15, 33]. The Ewald summation is used to deal with the long range Coulomb interaction and the Lennard-Jones interaction between water molecules is cut off at 9.0 Å. The interactions between water molecules and SWCNTs are contributed only by the Lennard-Jones potential between the oxygen and carbon atoms[18], which can be written as

$$U_{oc} = 4\epsilon_{oc} \sum_{i=1}^{N_o} \sum_{j=1}^{N_c} \left[\left(\frac{\sigma_{oc}}{r_{ij}} \right)^{12} - \left(\frac{\sigma_{oc}}{r_{ij}} \right)^6 \right], \quad (1)$$

where N_o is the total number of oxygen atoms, N_c is the total number of carbon atoms, and r_{ij} is the distance between the oxygen and carbon atoms. The parameters are taken as $\epsilon_{oc} = 0.1029$ kcal mol⁻¹ and $\sigma_{oc} = 3.280$ Å, obtained from Lorentz-Berthlot combining rules of $\epsilon_{oc} = \sqrt{\epsilon_{oo} \times \epsilon_{cc}}$ and $\sigma_{oc} = (\sigma_{oo} + \sigma_{cc})/2$. The parameters, $\epsilon_{oo} = 0.1549$ kcal mol⁻¹ and $\sigma_{oo} = 3.154$ Å are taken from the TIP4P model, $\epsilon_{cc} = 0.06835$ kcal mol⁻¹ and $\sigma_{cc} = 3.407$ Å are taken from multiple-shell fullerenes and multiwalled carbon nanotubes[34, 35]. To speed up MD simulations, we assumed that the carbon atoms on SWCNTs are distributed continuously, which is well known as the continuum model and has been used in a lot of systems [36]. Thus the potential between one oxygen atom and a SWCNT is written as

$$U(r) = n_d \int u(x) d\Sigma, \quad (2)$$

where r and x represent the distances of the oxygen atom to the axis of SWCNT and the surface element $d\Sigma$, re-

*Electronic address: jdong@nju.edu.cn

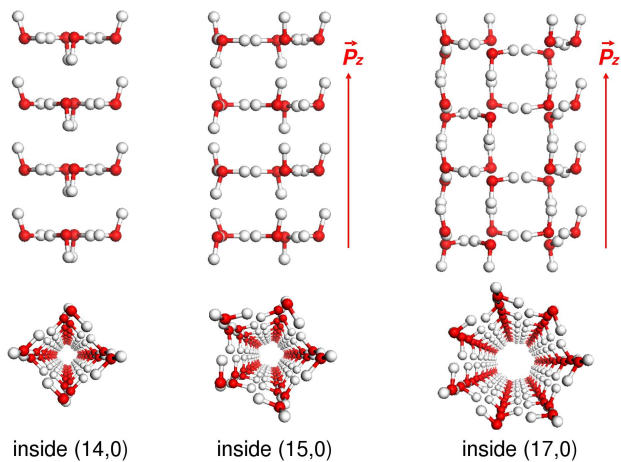


FIG. 1: (color online) Relaxed structures of ice nanotubes inside SWCNTs. The red and gray balls denote oxygen and hydrogen atoms, respectively. The ice nanotubes inside (15,0) and (17,0) SWCNTs have spontaneous electric polarizations along its axis direction. The polarization vectors are illustrated by \vec{P}_z and arrows.

spectively. n_d is the mean surface density of atoms on SWCNT [37, 38]. The C-C bond length of SWCNTs is assumed to be 1.42 Å. We checked the difference between the formula (1) and (2) is within 2% in our simulation conditions.

The MD simulations are performed by a modified TINKER package [39], in which the velocity-Verlet algorithm for integration of equation of motion and the Berendsen thermostat algorithm are used. The time step is set to be 0.5 fs. The motion of translation and rotation of the whole water molecules are eliminated during the MD simulations to calculate temperature. The simulation box is taken as a $50\text{Å} \times 50\text{Å} \times L$ cubic box, where L is the length along the axis of SWCNT. The periodic boundary conditions along the axis are used. Then, the real axial-pressure (P_{zz}) is the original calculated value times 2500 $\text{Å}^2/S$, where S is the area of the cross section of SWCNT.

Following Koga *et al.* [13, 14, 15], we first simulated water inside SWCNTs at constant temperature (T) and P_{zz} by using NPT assemble. We chose a high axial-pressure ($P_{zz}=200\text{MPa}$) condition and four types of zigzag SWCNTs, which are (14,0), (15,0), (16,0), and (17,0) with diameters of 10.96 Å, 11.74 Å, 12.53 Å, and 13.31 Å, respectively. During our MD simulations, the temperature was lowered stepwise starting from 450K to 100K and then heated stepwise back. The MD simulation time at each temperature is 2ns (10ns or more near the phase transition point). Some relaxed structures of the ice nanotubes and the polarized directions are both shown in Fig.1. These results consistent with those of Koga *et al.*[13, 14, 15, 16]. As illustrated in Fig.1, the ice nanotubes have 4, 5, and 7 side faces corresponding to inside (14,0), (15,0), and (17,0) SWCNTs, respectively. The ice nanotube inside (16,0) has 6 side faces but not shown in Fig.1. From the viewpoint of application, we

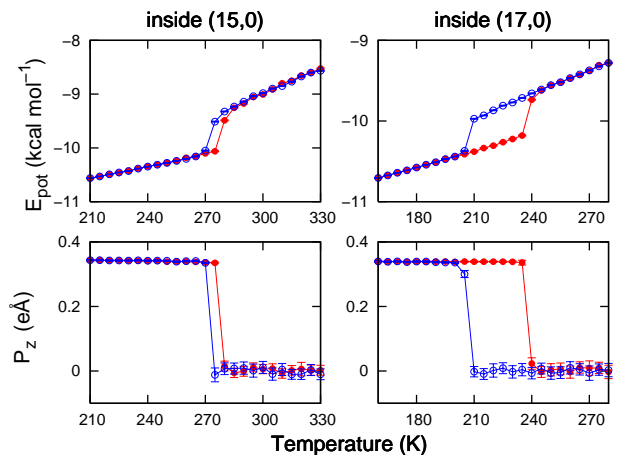


FIG. 2: (color online) The potential energy per water molecule (E_{pot} , in which the water-SWCNT interaction energy is excluded) and polarization per layer (P_z) versus temperature. The left and right panels are of the ice nanotubes inside (15,0) and (17,0) SWCNTs, respectively. The red filled circles and blue unfilled circles indicate the heating and cooling processes, respectively. The statistic standard errors are shown by the error bars, and lines are to guide the eye.

think that water or ice will probably be enclosed inside SWCNTs to produce Q1D devices. So, our later MD simulations were performed at constant T and volume (V or L), known as NVT assemble. The initial densities are taken by considering the results at high P_{zz} . In our simulations, the L is taken as 109.2 Å and the total number of water molecules in the simulation box is $40 \times n$, where n is the number of side faces and refers 4, 5, 6 and 7 corresponding to the four types of ice nanotubes inside (14,0), (15,0), (16,0), and (17,0) SWCNTs. The relaxed structures of the ice nanotubes and the polarized direction are almost the same as those at high P_{zz} shown in Fig.1. It is found that the ice nanotubes with odd number of side faces are ferroelectric, while those with even number of side faces are antiferroelectric. The polarizations of the relaxed ice nanotubes with $n=5$ and 7 are 0.351 eÅ and 0.347 eÅ per layer of water molecules. If we take a bundle of these ferroelectric “fibers” arranged in a dense packed hexagonal 2D lattice with a interspace distance of 3.4 Å (the same distance as that in graphite), the polarized rates are 0.15 C m⁻² and 0.12 C m⁻², respectively (the rate of BaTiO₃ is 0.26 C m⁻²).

The potential energy (E_{pot}) and spontaneous electric polarization along axis (\vec{P}_z) versus T of two ferroelectric ice nanotubes are plotted in Fig.2. It is found that the ferroelectric-paraelectric of the ice nanotubes strongly depends on the solid-liquid phase transition. The ferroelectric phase transition behavior of the ice nanotubes is much different from traditional ferroelectric bulk materials such as BaTiO₃, whose transition occurs at solid state phase and obeys the Curie-Weiss law. As an order parameter, the P_z of an ice nanotube drops at the solid-liquid phase transition point consisting with its $E_{\text{pot}}-T$

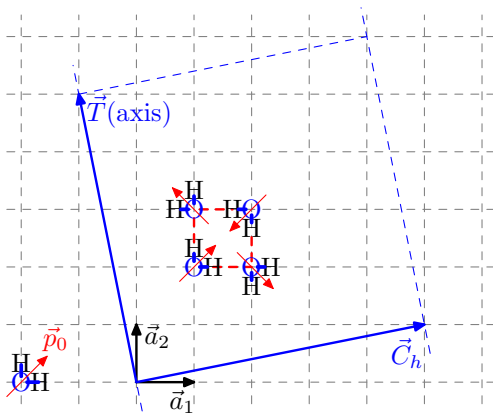


FIG. 3: (color online) Sketch of an unrolled 2D ice sheet, in which, the basis vectors (\vec{a}_1 and \vec{a}_2), the chiral vector (\vec{C}_h), and the axis vector (\vec{T}) are shown. $\vec{C}_h = n\vec{a}_1 + m\vec{a}_2$ corresponds to a $\langle n, m \rangle$ ice nanotube. The “Bernal-Cowler-Pauling bulk ice rule” is that every water molecule serves as a double donor and a double acceptor of hydrogen bonds, and every water molecule is hydrogen-bonded to exactly four nearest-neighbor molecules[1, 2]. In the 2D ice sheet and ice nanotube, the “ice rule” is still satisfied and the water network looks like a chessboard consisting of many square lattices. The square hydrogen-bond network is denoted in dashed lines and the details of the hydrogen bonds are shown at the center by four water molecules. The red arrow at a site denotes the dipole moment of a water molecule and is to direct its orientation. The example ice nanotube in this figure is $\langle 5, 1 \rangle$.

curve. This ferroelectric-paraelectric phase transition is a first-order transition coupled with violent structural change. The ferroelectricity is due to the special structures of ice nanotubes and the orientations of water molecules, which details are discussed as follows.

Just like for SWCNTs, we can analyze the structure of an ice nanotube by rolling a 2D ice sheet. For simplicity, we use a right-angle water molecular model to describe the 2D ice sheet. As illustrated in Fig.3, a 2D ice sheet consists of many square lattices and an ice nanotube can be described by a pair of numbers $\langle n, m \rangle$. By using this description, the three ice nanotubes shown in Fig.1 can be denoted as $\langle 4, 0 \rangle$, $\langle 5, 0 \rangle$, and $\langle 7, 0 \rangle$, respectively. A pair of $\langle n, m \rangle$ can describe the main frame of water network of an ice nanotube but fail to describe the orientations of water molecules. If we use the dipole moment of a water molecule \vec{p}_0 (0.45 eÅ in the TIP4P model and 0.38 eÅ in experiment) to direct its orientation, we can get another equivalent description of the “ice rule” in a 2D ice sheet and so in an ice nanotube: the projections of all dipole moments aligned along the basis vectors (\vec{a}_1 and \vec{a}_2 in Fig.3) must be in the same direction. That is to say, there are only two types of orientation for two nearest water molecules, parallel or perpendicularly.

To understand why the water molecules prefer the orientations shown in Fig.1, a very simple model is used to compare the energies of different isomers. We take the approximation: $E_n \simeq E_{LJ} + E_{HY} + E_P$, here E_{LJ} is

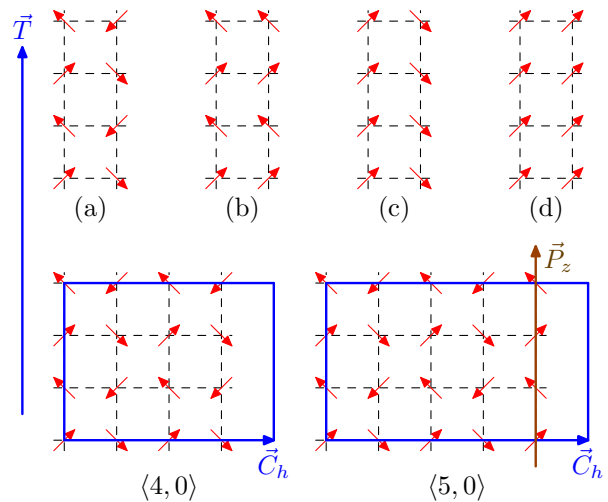


FIG. 4: (color online) The upper panel: four types of orientations of water molecules consisting one side face in a $\langle n, 0 \rangle$ ice nanotube; The lower panel: unrolled 2D hydrogen-bond network of two example ice nanotubes, $\langle 4, 0 \rangle$ and $\langle 5, 0 \rangle$. The red arrows indicate the orientations of water molecules as show in Fig.3. The potential energies of (a), (b), (c) and (d) are in increasing order, so the type (a) is preferred. A $\langle 4, 0 \rangle$ ice nanotube has 4 water molecules per layer with 2 upwards and 2 downwards, so it has no polarization at every layer. Every layer of a $\langle 5, 0 \rangle$ ice nanotube has 5 water molecules with 3 upwards and 2 downwards and has a polarization along the axis due to the one redundant upward water molecule. All the layers have the same directions of polarization along the axis since the “ice rule” forbids any opposite one. The “ice rule” accumulates the polarizations at every layer and generates a whole spontaneous electric polarization \vec{P}_z along the axis. The blue boxes are to denote the unit cell.

the Lennard-Jones potential, E_{HY} is the potential owned by hydrogen bonds, and the E_P is the potential due to dipole-dipole interaction which can be written as

$$E_P = \frac{1}{4\pi\epsilon_0} \sum_{ij} \frac{\vec{p}_i \cdot \vec{p}_j - 3(\hat{r}_{ij} \cdot \vec{p}_i)(\hat{r}_{ij} \cdot \vec{p}_j)}{|\vec{r}_{ij}|^3}, \quad (3)$$

where ϵ_0 is the permittivity of space, \vec{p}_i and \vec{p}_j are the dipole moments of water i and j , respectively. \vec{r}_{ij} is the displacement from water i to j , and \hat{r}_{ij} is its unit vector. For the first order approximation, the summation is over all nearest-neighbor sites. Although it might overestimate E_P , it can give us a clearer qualitative physical picture. The E_{LJ} and E_{HY} terms lead to the “ice rule” and decide the main frame of hydrogen-bond network. The E_P term due to dipole moments is much smaller than the other two terms but has an effect on the orientation of water molecules. At the same basis vectors (assuming $|\vec{a}_1| = |\vec{a}_2| = r_0$), different isomers with different orientations of water molecules have the same E_{LJ} and E_{HY} but different E_P , which makes us compare the E_P term only. A pair of perpendicular water molecules are $p_0^2/4\pi\epsilon_0 r_0^3$ lower in energy than a pair of parallel ones, so the orientations of two nearest water molecules prefer

the perpendicular type.

Now, we discuss why only the ice nanotubes with odd number of side faces possess ferroelectricity. We first classify a local water network to four types if we just consider the nearest pairs of water molecules. The upper panel of Fig.4 shows an example of the side faces of a $\langle n, 0 \rangle$ ice nanotube. The type (a) has the lowest energy without polarization and is preferred when an ice nanotube is formed. The type (b) is polarized along the axis although in a small higher energy. The potential energy differences between the four types are very small. As an example of $\langle 4, 0 \rangle$ ice nanotube, the type (b) is only 4.8×10^{-2} kcal mol $^{-1}$ (2.1×10^{-3} eV) per water molecule higher in energy than type (a). The lower panel of Fig.4 illustrates why a $\langle 5, 0 \rangle$ ice nanotube is ferroelectric while a $\langle 4, 0 \rangle$ ice nanotube is antiferroelectric. The reason is that a $\langle 5, 0 \rangle$ ice nanotube has one ferroelectric side face of type (b) while a $\langle 4, 0 \rangle$ ice nanotube has only antiferroelectric side faces of type(a). This consideration can be easily extended to other ice nanotubes. The origin of this type of ferroelectricity is the Q1D confinement and the orientational order of hydrogen bonds. We get the conclusion that, an ice nanotube with odd number of side faces has at least one redundant polarized water molecule at every layer and the “ice rule” accumulates them along the axis and generates a whole spontaneous electric polarization.

It is worthy to mention that, during our MD simulations, many fast quenched ice nanotubes exhibit fer-

roelectricity whatever odd or even number of side faces, which lie in small higher energies than those shown above. The side faces of these isomers are mainly type (b) and very stable at ice phase. So, if we apply an external electric field and cool the water fast, we might get ice nanotubes with larger polarization than those shown in this paper. It is also found that some $\langle 5, 0 \rangle$ and $\langle 7, 0 \rangle$ ice nanotubes with defects are slightly helix and ferroelectric too. In experiment, the orientations of water molecules can be detected by neutron scattering or infrared spectra, and the ferroelectricity can be reflected by second-order nonlinear optical coefficients.

In summary, ice nanotubes inside SWCNTs with odd number of side faces can exhibit ferroelectricity. These nanoscale Q1D ferroelectric fiber structural materials are different from traditional ferroelectric bulk materials both in ferroelectric-paraelectric phase transition behavior and the original mechanism. They may be applied in many fields, such as high sensitive sensors, nanoscale electric machines, nonvolatile memory devices, and so on. In addition, the similar type of ferroelectric mechanism probably exists in other nanoscale porous materials.

The authors thank Professor Ponder of Washington University for his kind offering of the TINKER package. This work was supported by the Natural Science Foundation of China under Grants No. 10474035 and No. A040108, and also from a Grant for State Key Program of China through Grant No. 2004CB619004.

-
- [1] J. D. Bernal and R. H. Fowler, *J. Am. Chem. Soc.* **1**, 515 (1933).
- [2] L. Pauling, *J. Am. Chem. Soc.* **57**, 2680 (1935).
- [3] J. C. Slater, *J. Chem. Phys.* **9**, 16 (1941).
- [4] S. M. Jackson and R. W. Whitworth, *J. Chem. Phys.* **103**, 7647 (1995).
- [5] X. Su, L. Lianos, Y. Shen, and G. A. Somorjai, *Phys. Rev. Lett.* **80**, 1533 (1998).
- [6] S. T. Bramwell, *Nature* **397**, 212 (1999).
- [7] H. Fukazawa *et al.*, *Astrophys. J.* **652**, L57 (2006).
- [8] L. D. Gelb *et al.*, *Rep. Prog. Phys.* **62**, 1573 (1999).
- [9] F. R. Hung *et al.*, *Appl. Phys. Lett.* **86**, 103110 (2005).
- [10] K. Koga, H. Tanaka, and X. C. Zeng, *Nature* **408**, 564 (2000).
- [11] N. E. Levinger, *Science* **298**, 1722 (2002).
- [12] H. Choe *et al.*, *Phys. Rev. Lett.* **95**, 187801 (2005).
- [13] K. Koga, R. D. Parra, H. Tanaka, and X. C. Zeng, *J. Chem. Phys.* **113**, 5037 (2000).
- [14] K. Koga, G. T. Gao, H. Tanaka, and X. C. Zeng, *Nature* **412**, 802 (2001).
- [15] K. Koga, G. Gao, H. Tanaka, and X. Zeng, *Pysica A* **314**, 462 (2002).
- [16] J. Bai *et al.*, *J. Chem. Phys.* **118**, 3913 (2003).
- [17] W. H. Noon, K. D. Ausman, R. E. Smalley, and J. Ma, *Chem. Phys. Lett.* **355**, 445 (2002).
- [18] G. Hummer, J. C. Rasaiah, and J. P. Noworyta, *Nature* **414**, 188 (2001).
- [19] T. Werder *et al.*, *Nano Lett.* **1**, 697 (2001).
- [20] R. J. Mashl, S. Joseph, N. R. Aluru, and E. Jakobsson, *Nano Lett.* **3**, 589 (2003).
- [21] D. J. Mann and M. D. Halls, *Phys. Rev. Lett.* **90**, 195503 (2003).
- [22] N. Naguib *et al.*, *Nano Lett.* **4**, 2237 (2004).
- [23] S. Sriraman, I. G. Kevrekidis, and G. Hummer, *Phys. Rev. Lett.* **95**, 130603 (2005).
- [24] A. Striolo, A. A. Chialvo, K. E. Gubbins, and P. T. Cummings, *J. Chem. Phys.* **122**, 234712 (2005).
- [25] E. Mamontov *et al.*, *J. Chem. Phys.* **124**, 194703 (2006).
- [26] A. Striolo, *Nano Lett.* **6**, 633 (2006).
- [27] A. I. Kolesnikov, J.-M. Zanotti, C.-K. Loong, and P. Thiyagarajan, *Phys. Rev. Lett.* **93**, 035503 (2004).
- [28] G. Reiter *et al.*, arXiv:cond-mat/0601072 (2006).
- [29] J. E. Spanier *et al.*, *Nano Lett.* **6**, 735 (2006).
- [30] A. V. Bune *et al.*, *Nature* **391**, 874 (1998).
- [31] C. H. Ahn, K. M. Rabe, and J. M. Triscone, *Science* **330**, 488 (2004).
- [32] W. L. Jorgensen *et al.*, *J. Chem. Phys.* **79**, 926 (1983).
- [33] M. Matsumoto, S. Saito, and I. Ohmine, *Nature* **416**, 409 (2002).
- [34] V. N. Popov and L. Henrard, *Phys. Rev. B* **65**, 235415 (2002).
- [35] J. P. Lu and W. Yang, *Phys. Rev. B* **49**, 11421 (1994).
- [36] H. Rafii-Tabar, *Phys. Rep.* **390**, 235 (2004).
- [37] L. A. Girifalco, M. Hodak, and R. S. Lee, *Phys. Rev. B* **62**, 13104 (2000).
- [38] G. Wu and J. M. Dong, *Phys. Rev. B* **71**, 115410 (2005).
- [39] P. Ren and J. W. Ponder, *J. Phys. Chem. B* **107**, 5933 (2003).